Five key lessons gained from induced seismicity monitoring in western Canada

Sepideh Karimi[1], Dario Baturan[1], and Emrah Yenier[1]

Abstract

In response to induced seismicity observed in western Canada, existing public networks have been densified and a number of private networks have been deployed to closely monitor induced earthquakes associated with oil and gas operations in the region. Over the past three years, we generated an unprecedented volume of seismic data from monitoring induced seismicity for some of the most active operators in western Canada. This rich data set can be used to understand preexisting geologic structures, the activation mechanisms and probabilities, and seismological attributes of the resultant ground motions. Acknowledging that the primary goal of private networks is assisting operators in making operational decisions, these insights can play key roles in improving the accuracy of event magnitudes, ground-motion predictions, and hazard estimates, which successively can be used for developing effective risk management strategies.

Introduction

An earthquake is a natural phenomenon resulting from the sudden release of tectonic stress accumulated over the years at an interlocking fault interface. Anthropologic activities such as mining, reservoir or dam impoundment, geothermal reservoir stimulation, wastewater injection, hydraulic fracturing (HF), or CO_2 sequestration can accelerate this natural process by changing the stress conditions, causing induced seismicity. In particular, earthquakes related to oil and gas production are predominantly small in magnitude, and are rarely felt locally or detected regionally. However, a number of such earthquakes with magnitudes M > 3 have been recorded in western Canada and in the United States since 2009. As a result, industry regulators have mandated some form of seismic monitoring near HF and wastewater disposal operations in some regions including British Columbia, Alberta, Ohio, and Oklahoma. Many private and shared seismic arrays have been deployed in response to these regulations and as part of operator seismic risk management programs. In addition, existing public networks have been densified. These efforts have resulted in an unprecedented volume of seismic data.

Recorded seismic data sets have value beyond regulatory compliance. These data sets can be used to aid in the identification of unmapped geologic structures, in the understanding of the correlation between operational parameters and observed seismicity, in the investigation of source attributes of induced earthquakes, and in the development of regional attenuation relationships that are required for accurate magnitude calculations and seismic hazard estimates. The findings of such studies can be used to guide operators and regulators in accurately assessing the risks associated with induced seismicity and in developing effective risk mitigation strategies (e.g., Bommer et al., 2015).

Over the past three years, we have worked with some of the most active operators in Canada, not only to meet mandated regulations but also to maximize the value of induced seismic monitoring (ISM) data sets. While supporting proactive risk management and regulatory compliance, we acquired several valuable insights that can assist with better management and understanding of the induced seismicity phenomenon: the importance of understanding the mechanisms of observed seismicity; the impact of monitoring resolution on data interpretation; the significance of calibrating magnitude equations and including ground motions in traffic light protocols (TLPs); and finally, the use of existing ISM data in evaluating the effectiveness of implemented risk mitigation protocols. The five lessons learned are summarized as follows.

Lesson 1: It is important to understand the nature of the seismicity

Induced seismicity in western Canada has close temporal and spatial correlation to HF operations. Most commonly, the recorded data sets show no baseline seismicity prior to the start of the operations, seismic activity that is uncorrelated to the HF stage times, recorded catalog *b*-values of ~1 (consistent with active tectonic regions), and residual seismicity that eventually diminishes hours or days following the HF completion. This type of seismicity is typically related to changes in the loading conditions (reduction in normal stress and/or increase in shear stress) introduced by fluid injection on proximal, unmapped faults. To result in events large enough to be detected by regional seismic networks, the fault must have a large potential rupture area, be located close to the stimulated wells, be optimally oriented within the current tectonic stress field, and be critically stressed.

Figure 1 shows an example data set that is typical of the described activation mechanism. The data were collected during a five-day, single-well HF operation in Alberta monitored by a local 11-station surface array located within 5 km of the wellhead. The array recorded 2321 events during the deployment, with magnitudes ranging from local magnitude of M_L −0.3 to M_L 2.8. The plan view of seismicity shows the delineation of six distinct preexisting structures, with north-northeast–south-southwest lineation, with no spatial correlation to the progression of the HF stages down the wellbore. Event focal depths are generally 250 m below the well lateral depth. The *b*-value computed for the entire catalog was 1.0, consistent with the Gutenberg-Richter relationship for natural seismicity. Three hundred fifty-six of the high signal-to-noise (S/N) events were used for moment-tensor (MT) inversion, with all solutions denoting a strike-slip mechanism striking north-northeast. Figure 1b also shows that the recorded seismicity had no temporal correlation to the HF stages, with less than 45% of activity recorded during the HF stage times. The seismicity ceased completely seven days following the completion.

[1]Nanometrics Inc.

https://doi.org/10.1190/tle37020107a1.1.

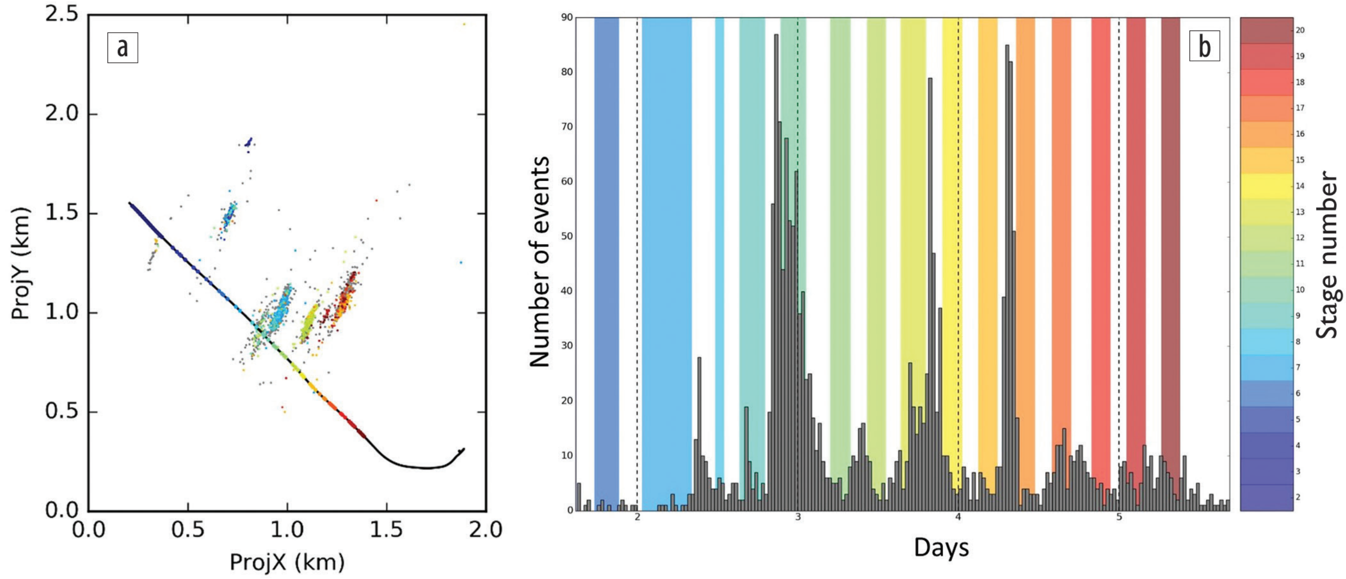

Figure 1. (a) Recorded seismicity related to single-well HF operation in Alberta. (b) Overlay of events histogram and HF stage time.

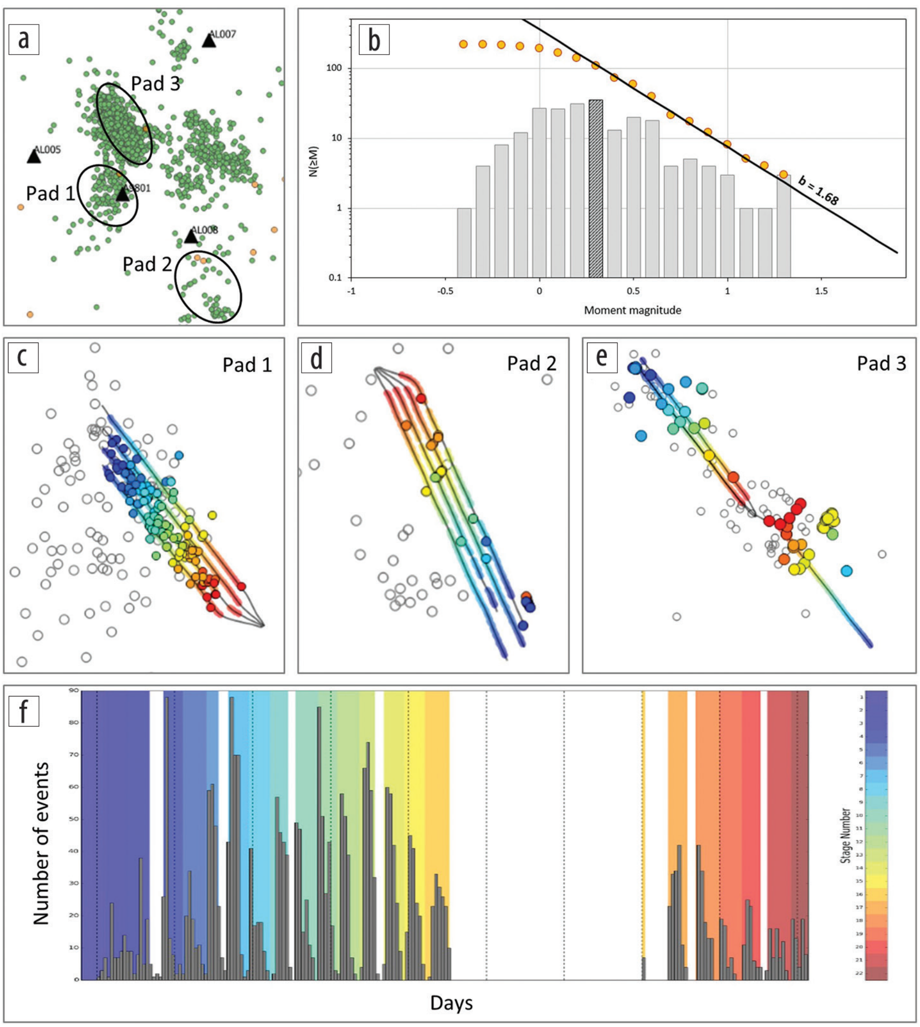

Figure 2. (a) Recorded seismicity related to a multipad HF site operated by Canbriam Energy in NEBC. Triangles represent locations of seismic stations in AOI. (b) Magnitude recurrence relationship for overall catalog (c–e) seismicity related to individual pads; hollow circles show the events location from ISM network and the color dots denote the events location using local network. Events are color coded based on the stage time. (f) Correlation of events histogram over time and HF stage time.

Although the data set shown in Figure 1 is typical of most HF-triggered seismicity in western Canada, there has been at least one case where the seismicity continued to be recorded for months after completion, suggesting different activation mechanisms. It is hypothesized that the triggering mechanism in that case was fluid diffusion across the fault via an existing hydrological connection between the induced HF network and the fault (Bao and Eaton, 2016). This activation mechanism is characterized by low fluid-recovery rates, as a large amount of fluid leaks off, pressurizing and "lubricating" the fault. This is more likely to occur if the fault is closer to the well laterals (i.e., tens or hundreds of meters). In this case, standard mitigation techniques, such as flowback or reduction in pumping rates and volumes, will have very little effect.

However, not all recorded induced seismicity is necessarily associated with fault activation. Figure 2 depicts a data set recorded as part of a passive seismic monitoring program of multipad HF operations carried out by Canbriam Energy in northeast British Columbia (NEBC). A local seismic network consisting of eight high-quality, three-component broadband seismometer stations detected a total of 1771 events within the operator area of interest (AOI) between April 2015 and January 2017. In addition to the backbone ISM network, dense microseismic monitoring arrays were deployed to monitor HF operations on individual pads. Figures 2c–e depict observed overlapping events located by the eight-station backbone array and dense microseismic arrays. The higher accuracy event location from microseismic arrays confirms no out-of-zone growth related to operations on all three pads. Figure 2f displays the correlation of HF stage time and seismicity rate related to pad 1 over time. The observation shows that more than 95% of the recorded activity occurs during HF stage time windows with no recorded seismicity before or after completions. Additionally, the examination of the magnitude recurrence attribute indicates a steep average *b*-value of 1.7 for the overall catalog (Figure 2b), with event magnitude ranges from M_L −0.4 to M_L 1.3, and *b*-value ranges from 1.5 to 2.3 for individual clusters. The observations therefore suggest that the seismicity is most likely associated with new stimulated rock volume, and reactivation of preexisting secondary fracture networks and small-scale features within the target zone. The implication then is that the activated features do not have the potential to cause larger magnitudes with possible felt intensity.

Lesson 2: What you can do with a data set depends largely on the recording network

Not all recording networks and the resulting data sets are created equal. Seismic monitoring networks involved with induced seismicity can be broadly grouped into four categories with escalating costs of deployment and operation: public (far regional) networks, regional subscriber arrays, private local (near regional) arrays, and microseismic arrays. The listed network types vary not only in operating mandate but also in terms of utilized instrumentation, deployment type, and network performance as measured by detected event location uncertainties and magnitude completeness (Mc) of the catalog. The monitoring resolution of the network ultimately governs how the resulting event catalogs are used. Table 1 summarizes the network performance and characteristics of each seismic network category.

Public networks. Seismic data collected by public networks are primarily used for public information, emergency response, and research purposes. Stations in these networks are typically spaced tens or hundreds of kilometers apart. The location uncertainty of the detected events is expressed in kilometers or tens of kilometers, with Mc in the M 1.8 to M 2.5 range. The depth of events detected by public networks is often fixed, as the solution is poorly constrained due to sparse network coverage. Despite the increased station density in areas where previous seismicity has been recorded, data from public networks are not a sufficient basis for operational decisions.

Regional subscriber arrays. Covering regulation designated monitoring regions, stations in regional subscriber arrays are typically spaced kilometers or tens of kilometers apart, and can cost-effectively support minimum regulatory compliance. The Mc is typically in the M 0.7 to M 1.8 range and varies based on the regional regulatory requirements. The networks are designed to have a Mc just below the regulation designated yellow traffic light threshold, with an event location uncertainty as low as 1 to 2 km.

Private local (or near regional) arrays. These arrays typically cover one or multiple pads owned by a single operator, with stations spaced about 2 to 5 km apart. The event location uncertainty of private local arrays is typically in hundreds of meters, making the data useful for fault mapping, detecting activation of preexisting secondary fracture networks, and risk management for regulatory compliance. With Mc ranging from about M −0.3 to M 0.7, these arrays can detect the lower magnitude events that are key to near-real-time evaluation of the effectiveness of risk mitigation protocols employed by the operators.

Microseismic arrays. These arrays are intended to provide high-resolution characterization of the HF-stimulated region on one or multiple wells from a single pad and encompass a variety of geometries. For example, large surface arrays utilize several thousand sensors deployed above the target region to detect and characterize microseismic activity. Alternatively, sparse surface arrays and shallow borehole arrays utilize tens rather than thousands of sensors leading to larger distances between sensors. Downhole surveys typically use one or more tool strings deployed in observation wells at depths near the target formation. The choice of specific monitoring geometry depends on the region and target.

For microseismic-monitoring arrays, location uncertainty is reduced to meters or tens of meters, Mc is in the M −2.0 to M −0.3 range, and consequently the microseismic data sets allow operators to evaluate their completions strategy effectiveness in addition to well spacing, and to characterize the stimulated region among others. Although microseismic arrays produce the highest resolution data sets, due to their cost, this is excessive for ISM purposes. Public, regional subscriber, and local arrays use broadband instruments to cover the anticipated large magnitude and recording distance range. Microseismic arrays, on the other hand, typically use surface or downhole geophones.

Figure 3 illustrates the differences in the performance of three seismic network types using a data set recorded near an active target HF pad in the Duvernay region of central Alberta. The Public Alberta Geological Survey (AGS) network detected a diffuse cloud of about 300 events, with Mc of M 2.3, using four real-time streaming stations within 200 km of the study area within a 21-month monitoring time (January 2015 to November 2016) (Figure 3a). Three times as many events were recorded within a smaller 16-month overlapping time window by a regional subscriber array deployed in response to Alberta Energy Regulator (AER) seismic monitoring requirements. The subscriber array consists of 12 semipermanent, shallow-buried seismometer stations located 5 to 110 km from the monitored pad. The Mc for the near regional array is M 1.1, and its data set brings more focus to the event clusters (Figure 3b). In comparison, a tenfold increase in the number of detected events was observed in the data set recorded by a local four-station network operating during the entire AGS recording time window. The Mc of the local array is 0.6 with improved monitoring resolution starting to delineate faults and small features in the area (Figure 3c).

Figure 3d illustrates the differences in epicenters for the events recorded by local, regional, and public arrays. For the 184 events recorded by both local and subscriber arrays, the epicenter shifts

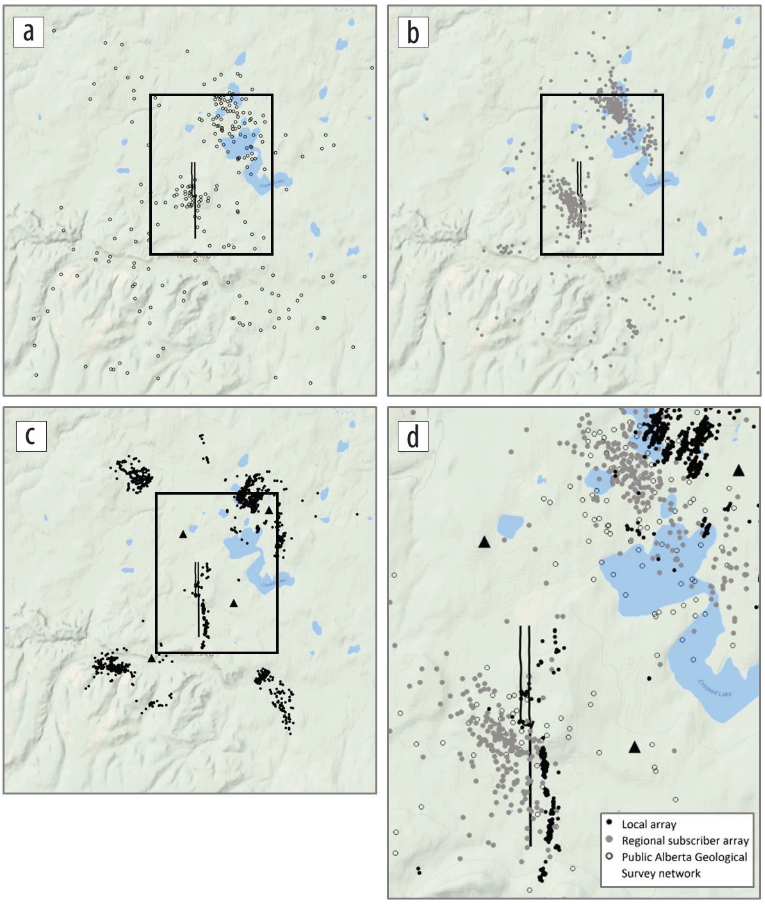

Figure 3. Network performance comparison using a data set recorded near an active target HF pad in the Duvernay region of central Alberta. (a) AGS network catalog. (b) Regional subscriber array catalog. (c) Local four-station array catalog. (d) Closer view of overlapping three-event catalogs adjacent to the well pad.

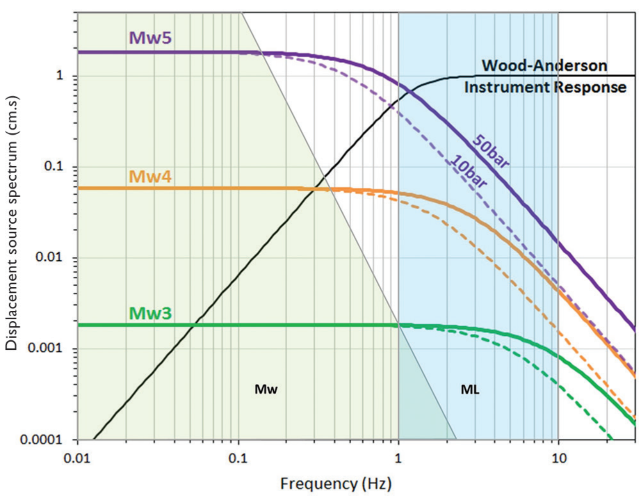

Figure 4. Frequency band of interest to calculate moment magnitude and local magnitude is shown on the displacement spectra of hypothetical earthquakes.

vary from 0 to 6.8 km (average 1.5 km). The differences between epicenters of 62 common events that were recorded by local and AGS arrays range from 0 to 11.2 km (average 2.7 km). These examples highlight that care must be taken in how the data are used, as the interpretation can change with an increase in the monitoring resolution.

Lesson 3: Sufficient data can significantly reduce magnitude uncertainty

Magnitude is the most publicly noted aspect of an earthquake besides its location. All TLPs introduced to date via regulations are based on staged magnitude thresholds. For example, the BC Oil and Gas Commission (BCOGC) (BCOGC, 2015) and the AER will issue a shutdown order at M 4.0 within the designated areas. To date, there have been three shutdowns due to induced seismicity in BC and two in Alberta.

Magnitude uncertainty is a known problem in earthquake seismology (Kao et al., 2016). The discrepancy is observed in the magnitude reported by different seismic networks, whether it is the result of using different magnitude scales that measure amplitudes in different frequency bands (Figure 4); uncalibrated, nonunique equations; inadequate instrumentation; or differences in recording seismic station placement and azimuthal coverage. There are many magnitude scales, with local magnitude (M_L) and moment magnitude (M_W) being predominantly used in ISM networks.

Local magnitude, which is the standard for local and regional seismic networks around the world, is easy to compute; but it is based on an amplitude reading at a single frequency, which means that this type of reported magnitude does not account for radiation pattern and can be affected significantly by local site amplification factors and regional attenuation attributes. Moment magnitude, which is the standard magnitude in microseismic monitoring, is related to physical properties of fault displacement and can account for radiation pattern if it is computed as part of a full MT inversion. However, it can be computationally expensive, and it requires knowledge of regional attenuation parameters (*Q* and geometrical spreading) and good S/N across the frequency band of interest.

Significant discrepancy has been observed in reported magnitudes for similar events recorded by multiple recording networks. For example, as indicated in Table 2, Natural Resources Canada reported M_L 4.4 for an event that occurred 23 January 2015 near Fox Creek, western Alberta. For the same event, a regionally calibrated local magnitude relation (Yenier, 2017) resulted in M_L 3.9, which is the same magnitude that was reported by USGS (Mb 3.9). The Pacific Geoscience Centre reported the magnitude of the event using regional MT (RMT) solution as M_W 3.7. Finally, the resulting moment magnitude calculated from spectral fitting approach was M_W 4.0.

Magnitude uncertainty can be reduced in many ways. Utilizing broadband instrumentation in ISM networks is critical to accurately capturing the amplitude and frequency content of the entire expected magnitude range. Maximizing the azimuthal coverage via data sharing and the inclusion of publicly available stations helps to average out the effects of radiation pattern and site amplifications. For M > 3.5 events, M_W magnitude determined from a MT inversion approach is preferred over M_L scale. This is because it minimizes the effects of site amplification by utilizing long-period data (typically 0.02 to 0.08 Hz) and accounts for the radiation pattern effects through focal mechanism inversion.

Local magnitude scale is typically used for events of M < 3 and is widely referenced in monitoring regulations (AER, 2015). This magnitude type is determined from peak amplitudes projected to a reference distance of 100 km (Richter, 1935, 1958). A proper distance correction that consistently reflects the regional attenuation attributes is a prerequisite for accurate M_L calculations. However, standard M_L relations derived from California data (e.g., Richter, 1935, 1958; Hutton and Boore, 1987; Eaton, 1992) are generally used in areas where seismic data are insufficient to examine attenuation effects. This may result in biased M_L values if the adopted magnitude relation does not comply with the attenuation characteristics of the target region. For instance, Yenier (2017) developed a regionally calibrated M_L formula for the Western Canada Sedimentary Basin (WCSB) using a rich ground-motion data set compiled from local and regional networks in the area (Figure 5). He found that standard M_L relations failed to capture the rates and shape of amplitude attenuation in the region, resulting in overestimated magnitudes by 0.3 to 0.6 units. The overestimation is larger for local networks due to the increased discrepancy between standard M_L relations and the actual attenuation properties at close distances (Figure 5b).

The importance of earthquake magnitudes is not limited to TLPs. Earthquake catalogs are the base for seismic hazard estimations; consequently, bias in magnitude calculations may potentially result in inaccurate hazard estimations. While different magnitude scales are reported by different agencies, moment magnitude is the most widely used type of magnitude in seismic hazard calculation. Relationships between different magnitude scales are not linear and are region dependent. The M_L-M_W relationship for events recorded near Fox Creek, Alberta is illustrated in Figure 5c (Yenier, 2017). The comparison indicates that M_W attains larger values than M_L for events with moment magnitude larger than 3.3. M_L, and M_W magnitudes show good agreement for larger events. The discrepancy between the two magnitude scales causes *b*-values that are computed from M_W magnitudes to be ~0.3 higher than *b*-values that are from M_L magnitudes (Yenier, 2017).

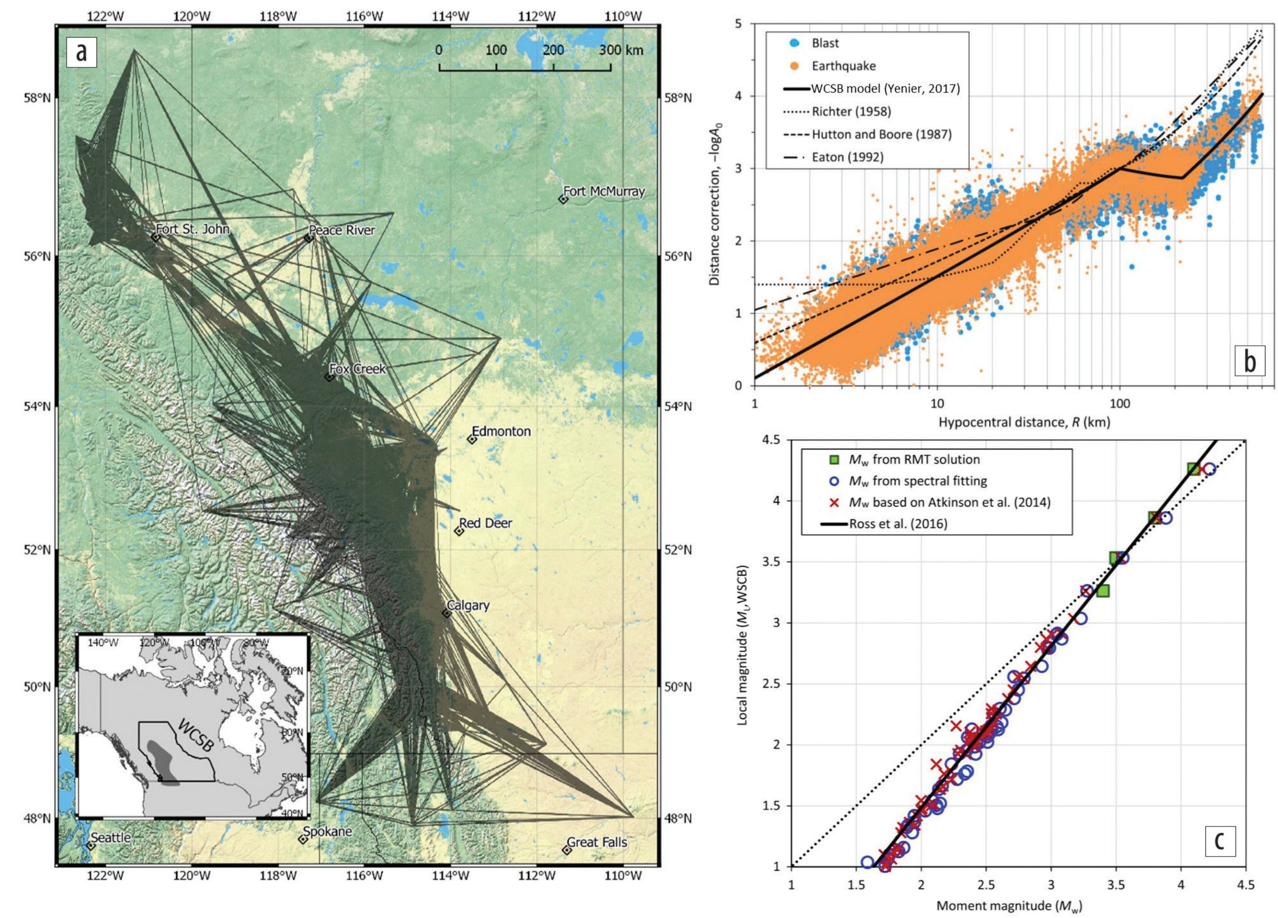

Figure 5. (a) Regional coverage of the surface projection of ray paths, for events used by Yenier (2017). (b) Regional distance correction model derived for WCSB by Yenier (2017) in comparison to those of standard M_L relations. Scatter dots indicate distance correction obtained from earthquake and mining blast recordings in WCSB. (c) Local magnitude and moment magnitude comparison for event recorded near Fox Creek, Alberta. The two magnitude scales are in good agreement for M_W > 3.3. Local magnitudes attain smaller values than moment magnitudes for such events. The discrepancy between the two increases with decreasing event size. From Yenier (2017).

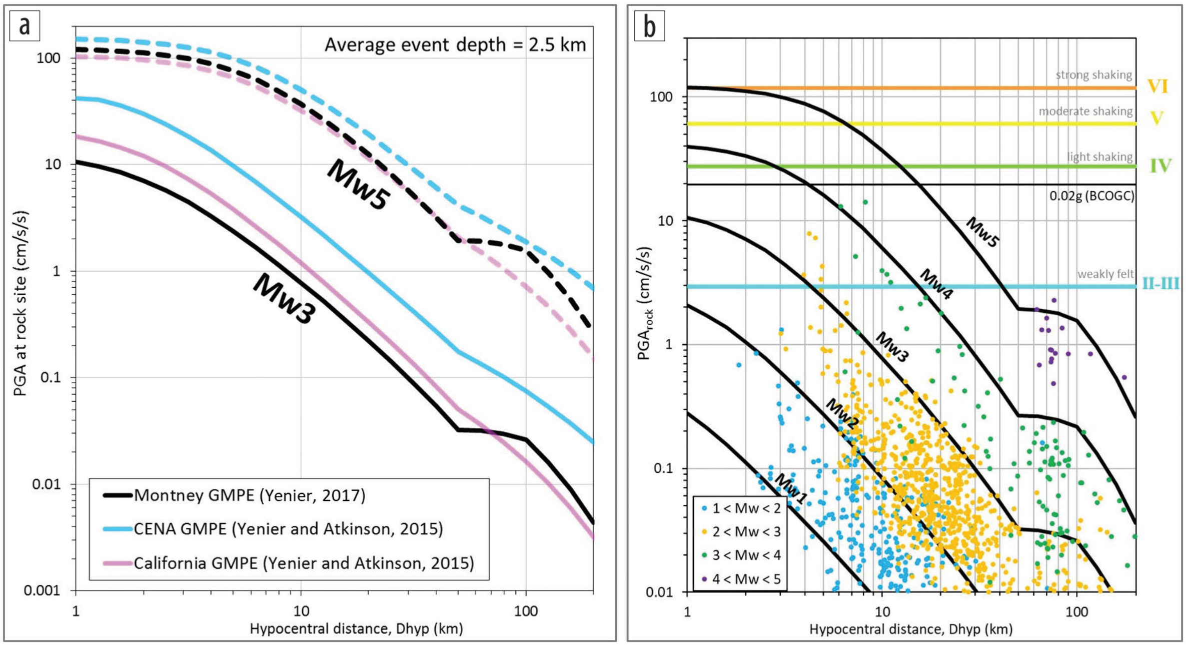

Figure 6. (a) Estimated peak ground acceleration (PGA) as a function of hypocentral distance for two magnitudes using three different GMPEs. Black lines show the local Montney GMPE. (b) PGA predictions at reference rock site condition, for different magnitude (black lines). Circles represent site effect corrected PGAs of events used in ground-motion modeling, color coded based on magnitude bins. Horizontal lines indicate level of ground motions for different shaking intensities, as labeled on the right. From Yenier et al. (2017).

Lesson 4: Ground motions should complement magnitudes in TLPs

Existing induced seismicity regulations use event magnitude as the controlling parameter of operational protocols by limiting the size of induced events in order to avoid public nuisance and potential damage. This is typically done by means of TLPs, where actions are required to be taken in response to staged magnitude thresholds. Although event magnitude is well correlated with ground-shaking intensity and damage potential, it is not the only controlling parameter. Two earthquakes with the same magnitude can result in different ground motions due to differences in source mechanism, stress drop, distance attenuation, and local site conditions. Ground motions are a more direct measure of an earthquake's impact because they implicitly account for the regional source, attenuation, and site effects. Therefore, ground motions can play a complementary role in TLPs, in addition to event magnitude. In this regard, BCOGC is the first regulatory body to adopt ground-motion-based regulations that require at least one accelerometer to be installed within 3 km of an active well, with a reporting threshold of 0.02g (BCOGC, 2016). During production of this paper, BCOGC reduced the reporting ground motion to 0.008g (BGOGC, 2017). The ground-motion data are not used to drive a TLP, instead they provide near-field large ground-motion data for research purposes.

The accurate estimation of ground-shaking intensities associated with induced earthquakes is a prerequisite for a successful adaptation of ground motions in existing TLPs. This can be done by using ground-motion prediction equations (GMPE) and site amplification models that are consistent with source, attenuation, and site attributes of the AOI. GMPEs define how ground-motion amplitudes scale with magnitude and distance in a region for a reference site condition (e.g., rock site). Existing published GMPEs are mostly defined from tectonic events and do not accurately capture the seismological attributes of induced events. Furthermore, such models average out subregional variations of attenuation and may not capture the path specific characteristics of the region in which the induced events occurred. Using an unsuitable model may introduce bias in estimates of ground motions and consequently seismic hazard.

Figure 6a shows results from a ground-motion project initiated by Canbriam Energy for induced events in NEBC (Yenier et al., 2017). It highlights the differences between local predictive models and published GMPEs for California and central and eastern North America (CENA). The local GMPE was developed using a hybrid approach, in which a magnitude scaling function obtained from stochastic point source simulations was calibrated against ground motions obtained from 180 local and near regional events. One observation is that induced events in NEBC attained lower ground motions than the shallow tectonic events in CENA but were similar to those in California. The local GMPE also accounts for a strong "moho-bounce" effect, which is observed at intermediate distances for events in NEBC.

As part of the earlier mentioned project, shake maps were generated for selected real and scenario induced earthquakes. This was done by supplementing the rock site ground-motion estimates from local GMPEs with local site amplification estimates from a generated map that accounts for the spatial variation of near-surface site effects on ground motions. This allowed for back calculation of minimum magnitude for critical events that may result in ground motions exceeding the felt, regulatory, or damage thresholds with a certain probability (Figure 6b). This process provides a science-based approach to enhancing the current magnitude-based TLPs with ground-motion estimates utilizing a locally developed GMPE and site amplification map.

Lesson 5: Risk mitigation protocols require high-resolution seismic monitoring

The goal of ISM networks is to help operators manage induced seismic risk and evaluate the effectiveness of their induced seismicity risk mitigation protocols. To date, the data in western Canada show that the conditions at individual pads are relatively unique in terms of in situ stress regime, the size of the potential rupture area and orientation, as well as the proximity to the well(s) being completed. It is therefore reasonable to assume that the same risk mitigation strategy may not work at each pad. Consequently, some form of seismic monitoring is required to provide real-time feedback on whether the mitigation protocol is influencing the likelihood of the occurrence of larger events.

Figure 7 illustrates an example of catalog level data products generated using a data set recorded by a four-station local seismic network monitoring HF operation over a two-year period near Crooked Lake, Alberta. The plots show the temporal variations in seismicity rate and *b*-value estimates in addition to recorded magnitudes for the five time windows surrounding significant events. The preliminary observations show some common seismicity traits for the study region. The observations show that in almost all cases the *b*-values are consistently below 1 prior to the occurrence of the larger events and that most of them follow the initial spike in the seismicity rate. The larger events are also preceded by many smaller magnitude events that occur along the same lineaments shown on the map view, indicating smaller segments of the fault slipping prior to the major rupture. Risk mitigation using catalog level data products, as shown in this example, is the focus of ongoing research with the goal of understanding the triggering mechanisms and identifying signs of high-risk fault activation in near real time.

However, we can now confirm, based on the monitoring results from western Canada to date, that local or near regional seismic network monitoring resolution along with advanced seismic data processing techniques is required to generate data sets that are rich and accurate enough to be used as inputs into such real-time risk indicators. The catalogs must be extensive with small-magnitude events well below yellow traffic light thresholds to compute catalog level data products such as *b*-value or seismicity rate variations accurately. In addition, the catalog earthquakes must be located accurately to delineate activated structures. Taken together and integrated with completion parameters in near real time, this information holds the key to near-real-time evaluation of the effectiveness of risk mitigation protocols developed by operators.

Discussion

Induced seismicity risk can be evaluated prior to drilling by detailed geologic and geophysical analysis of seismic survey data to characterize the preexisting structures and potential fluid pathways to those structures. Drilling and completion programs can then be designed to minimize the likelihood of proximal faults activation and large magnitude event occurrence. However, as data recorded to date in western Canada have shown, most of the activated faults are unmapped, and the conditions (in situ stress state, fault proximity, area, and fault orientation) at each pad are highly variable.

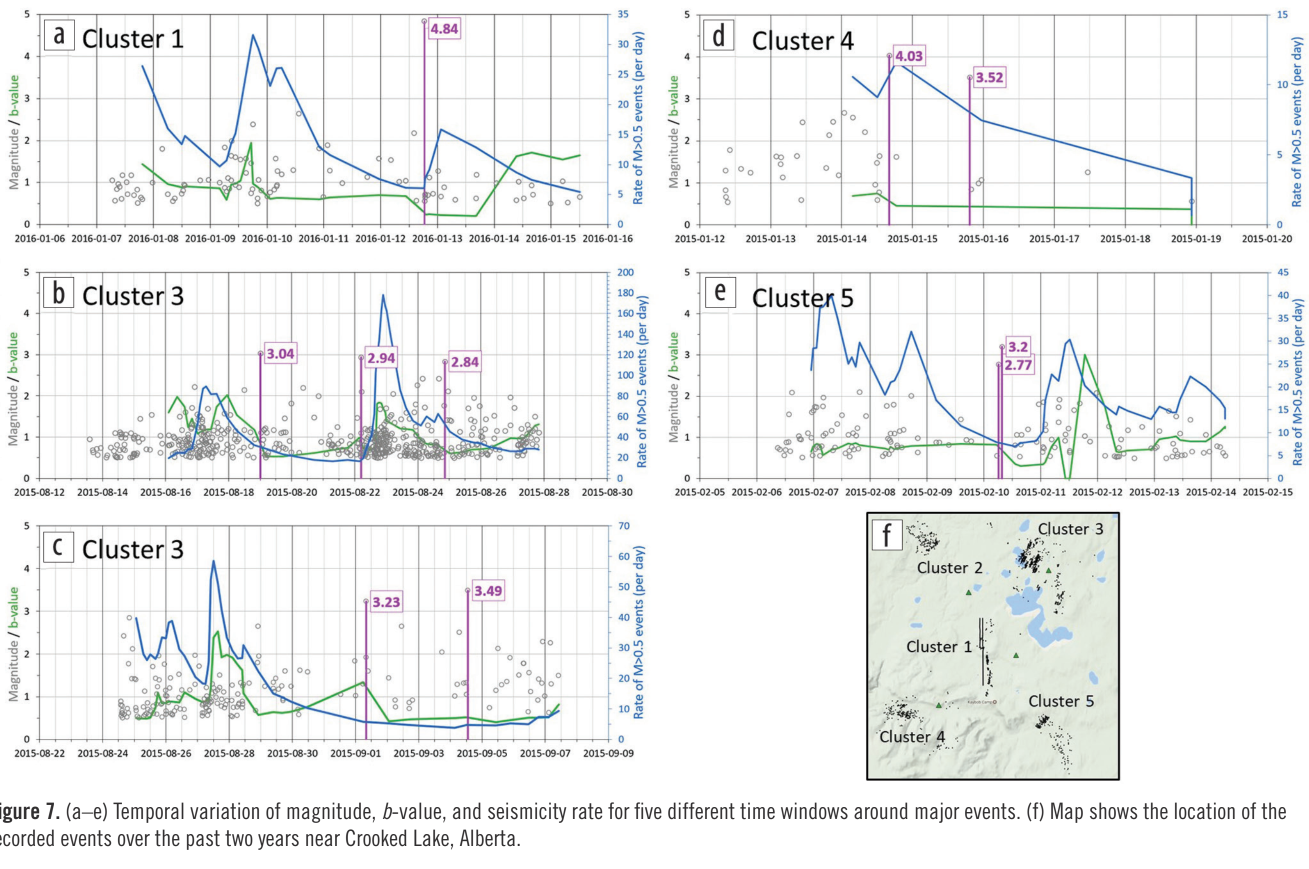

Figure 7. (a–e) Temporal variation of magnitude, *b*-value, and seismicity rate for five different time windows around major events. (f) Map shows the location of the recorded events over the past two years near Crooked Lake, Alberta.

This is witnessed by the observation of different activation mechanisms and the presence, in some cases, of seismicity that is not associated with faults. These observations highlight the importance of some form of real-time seismic monitoring in understanding, evaluating, and managing the seismic risk in near real time.

Observed data have also shown the importance of accounting for recording uncertainty when interpreting the seismic monitoring results. Often the interpretation changes once the seismic monitoring resolution increases and lower uncertainty data become available. It is therefore important to understand the limitations and the role of each monitoring network and to use the data accordingly.

The uncertainty and discrepancy in magnitude estimates is critical, as all TLPs introduced to date are magnitude based and can incur high costs associated with operational shutdowns. Furthermore, bias in magnitude calculation can result in a potential bias in seismic hazard estimations. The high volume of data recorded to date from private and public arrays allow these challenges to be overcome by calibrating the existing equations to reflect the attenuation attributes of the regions in which these equations are applied, references to specific calibrated equations in regulations, data sharing, and use of RMT solutions for large events to minimize the effects of site amplification, azimuthal coverage, and radiation pattern in magnitude estimates.

Another way to address magnitude limitations is to extend TLPs to include ground-motion recordings. Ground motions provide better connection to the shaking perception, damage potential, and actual risk associated with triggered events. Existing monitoring protocols for mining explosions where ground-motion recorded data are driving the decision (OSM, 1986) can provide some guidance. In these protocols, the installation of a three-component seismograph and decision making based on recorded frequency-based peak particle velocity provide a more robust risk management portfolio. Unlike magnitudes, ground motions are directly measured by instruments deployed at the locations of interest, such as populated areas or important infrastructure. Recorded ground motions and estimated values from empirically derived GMPEs provide a link to the true impact of events as ground motions account for regional variations in attenuation, site amplifications, and recorded seismicity attributes (stress drop, depth, and slip mechanism).

Finally, seismic monitoring can be used to recognize the signs of fault activation during operation in near real time and assist in risk management by potentially providing a measure of whether the adjustments in HF completion parameters or changes in injection rate and volume of the fluids in wastewater disposal operations are influencing the likelihood of large magnitude event occurrence. In this respect, high-monitoring resolution with Mc well below yellow TLP thresholds is critical. The use of denser (local or near regional) seismic networks combined with near-real-time implementation of advanced seismic processing techniques is a prerequisite for accurate interpretation of observed seismicity in near real time and better understanding and management of the induced seismicity phenomenon via research. TLE

Corresponding author: sepidehkarimi@nanometrics.ca

Acknowledgments

We are grateful to our colleagues at Nanometrics Inc. for their support and contribution to this study. In particular, we would like to thank Andrew Reynen, Kit Chambers, Mairi Miller, and Christine Cowtan. We thank Nahanni McIntosh for her involvement in an earlier version of the manuscript. We are thankful to Steve Brown and Heather DeShon for the insightful comments and constructive feedback that greatly improved the manuscript. We would like to acknowledge Canbriam Energy and Repsol for granting permission to publish on data obtained from their local networks.

References

Alberta Energy Regulator, 2015, Duvernay subsurface order no. 2, https://aer.ca/data-and-publications/orders/subsurface-orders, accessed 28 December 2017.

Bao, X., and D. W. Eaton, 2016, Fault activation by hydraulic fracturing in western Canada: Science, **354**, no. 6318, 1406–1409, https://doi.org/10.1126/science.aag2583.

Bommer, J. J., H. Crowley, and R. Pinho, 2015, A risk-mitigation approach to the management of induced seismicity: Journal of Seismology, **19**, no. 2, 623–646, https://doi.org/10.1007/s10950-015-9478-z.

British Columbia Oil and Gas Commission, 2015, Industry bulletin 2015–32.

British Columbia Oil and Gas Commission, 2016, Guidance for ground motion monitoring and submission.

British Columbia Oil and Gas Commission, 2017, Guidance for ground motion monitoring and submission.

Eaton, J. P., 1992, Determination of amplitude and duration magnitudes and site residuals from short-period seismographs in northern California: Bulletin of the Seismological Society of America, **82**, no. 2, 533–579.

Hutton, L. K., and D. M. Boore, 1987, The M_L scale in southern California: Bulletin of the Seismological Society of America, **77**, no. 6, 2074–2094.

Kao, H., D. W. Eaton, G. M. Atkinson, S. Maxwell, and A. Babaie Mahani, 2016, Technical meeting on the traffic light protocols (TLP) for induced seismicity: Summary and recommendations: Geological Survey of Canada, https://doi.org/10.4095/299002.

OSM blasting performance standards, 30 code of federal regulations, 1986, sec. 816.61.

Richter, C. F., 1935, An instrumental earthquake magnitude scale: Bulletin of the Seismological Society of America, **25**, no. 1, 1–32.

Richter, C. F., 1958, Elementary seismology: W. H. Freeman and Co., 578 p.

Structure response and damage produced by ground vibration from surface mine blasting, USBM RI 8507.

Yenier, E., 2017, A local magnitude relation for earthquakes in the Western Canada Sedimentary Basin: Bulletin of the Seismological Society of America, **107**, no. 3, 1421–1431, https://doi.org/10.1785/0120160275.

Yenier, E., D. Baturan, B. Bialowas, B. Batlai, and J. Nieto, 2017, Induced-seismicity risk-mitigation strategies: Montney case study: 87th Annual International Meeting, SEG, Expanded Abstracts, 5345–5349, https://doi.org/10.1190/segam2017-17785730.1.